

Hydrogen sulphide release to surface waters at the Precambrian/Cambrian boundary

Martin Wille¹, Thomas F. Nägler¹, Bernd Lehmann², Stefan Schröder³† & Jan D. Kramers¹

Animal-like multicellular fossils appeared towards the end of the Precambrian, followed by a rapid increase in the abundance and diversity of fossils during the Early Cambrian period, an event also known as the 'Cambrian explosion'^{1–3}. Changes in the environmental conditions at the Precambrian/Cambrian transition (about 542 Myr ago) have been suggested as a possible explanation for this event, but are still a matter of debate^{1–3}. Here we report molybdenum isotope signatures of black shales from two stratigraphically correlated sample sets with a depositional age of around 542 Myr. We find a transient molybdenum isotope signal immediately after the Precambrian/Cambrian transition. Using a box model of the oceanic molybdenum cycle, we find that intense upwelling of hydrogen sulphide-rich deep ocean water best explains the observed Early Cambrian molybdenum isotope signal. Our findings suggest that the Early Cambrian animal radiation may have been triggered by a major change in ocean circulation, terminating a long period during which the Proterozoic ocean was stratified, with sulphidic deep water.

Trace-metal records, especially the molybdenum (Mo) isotopic record, are increasingly used as a proxy for changing redox conditions in the oceans^{4–6}. Mo is highly soluble and unreactive under oxic conditions, but is easily incorporated into sediments under highly euxinic conditions. Specifically, the Mo isotopic seawater record as deduced mainly from euxinic sediments reflects the relative global amount of euxinic Mo sedimentation and, therefore, the redox condition of the oceanic environment. Thus, Mo signatures in black shales of the Precambrian/Cambrian (PC/C) transition can provide insight into the redox condition of the ocean during that period. Here we present and compare Mo isotopic signatures from black shales of the Ara Group, Oman^{7,8}, and from the Niutitang Formation, Yangtze Platform, China⁹, and examine their global significance (Fig. 1). The Ara Group contains an ash bed within the basal strata of the A4 carbonate bed, dated to 542.0 ± 0.3 Myr ago³, which is correlative to the base of the black shales studied here. The Chinese black shale sequence of the Niutitang Formation has a basal sulphide marker bed with an Re–Os age of 541 ± 16 Myr (ref. 10). The correlation of the two profiles is further corroborated by the globally recorded negative carbon isotopic excursion at the PC/C boundary^{3,11}.

Samples from the Chinese sulphide marker bed from different localities, with extreme Mo concentrations up to 7 wt%, show a homogeneous Mo isotopic signal of around $1.1\delta^{98/95}\text{Mo}$ (where $\delta^{98/95}\text{Mo}$ denotes the parts-per-thousand deviation of the $^{98}\text{Mo}/^{95}\text{Mo}$ ratio relative to the J&M Mo standard). The same overall Mo isotopic signal is also found in black shales stratigraphically above the sulphide marker bed at much lower Mo concentrations. Although hydrothermal circulation has been proposed as a source for metal enrichment¹², the homogeneous isotopic composition over a large Mo concentration range can only originate from a single, isotopically

homogeneous Mo source⁹. A similar overall Mo isotopic composition of $1.2\delta^{98/95}\text{Mo}_{\text{J&M standard}}$ is found in the Early Cambrian black shales from Oman, lending support to the interpretation of sea water being the main source of the Mo signal in both basins.

Mid-Proterozoic-era Mo isotopic signatures show similar values and are interpreted as evidence for widespread anoxia in the deep mid-Proterozoic oceans⁶. Our new Early Cambrian data support the idea that this ocean redox stratification was long-lasting. If the Mo source of the metal-enriched sulphide layer at the PC/C boundary is the Mo sea water inventory⁹, then the Mo-scavenging mechanism involved cannot be the same as that responsible for metal enrichment in recent euxinic sediments, where increased total organic carbon supply is considered as the main driving mechanism¹³. The total organic carbon concentrations within the Chinese sulphide marker bed are similar to those of normal black shales (~ 10 wt%), whereas the Mo concentrations are several orders of magnitude higher.

The transformation from molybdate to thiomolybdate in the presence of H_2S is a highly efficient Mo-scavenging process¹⁴. However, the supply of molybdate to the anoxic water mass is equally important for Mo enrichment¹³. The high Mo concentrations found in the Chinese marker bed require both excessive H_2S concentration and sufficient molybdate supply. The mixing of euxinic, H_2S -rich bottom waters with molybdate-rich surface waters in an upwelling regime

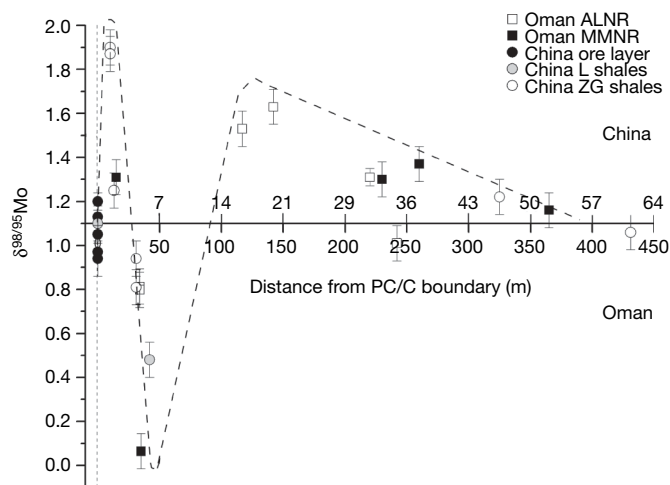


Figure 1 | Merged Mo transient signal of Early Cambrian black shales from the Yangtze Platform and Oman basin. Oman MMNR and Oman ALNR represent black shales from intermediate and deep basins wells, respectively⁷. Chinese ZG and L shales are from the Niutitang Formation (ZG taken at Ganziping, L taken at Yuanling)⁹. Error bars show the external standard reproducibility of $0.1\delta^{98/95}\text{Mo}$ if measured uncertainties are lower.

¹Institute of Geological Sciences, University of Bern, Baltzerstrasse 3, 3012 Bern, Switzerland. ²Institute of Mineralogy and Mineral Resources, Technical University of Clausthal, 38678 Clausthal-Zellerfeld, Germany. ³Earth, Atmospheric and Planetary Sciences, Massachusetts Institute of Technology, Cambridge, Massachusetts 02139, USA. †Present address: Total E&P, Avenue Larribau, F-64018 Pau, France.

could thus be a reasonable explanation for the extreme metal enrichment found in the Chinese sulphide marker bed and other localities¹⁵. Additionally, the redox-sensitive elements such as uranium and vanadium also show enrichments in both basins at the PC/C boundary (see Supplementary Information) and provide evidence for euxinic conditions in both basins¹⁶.

Further evidence for such an explanation comes from Mo isotopic signatures of black shales immediately above the PC/C boundary, which in both basins show the largest offset from the overall homogeneous Mo isotopic composition of $\sim 1.1\delta^{98/95}\text{Mo}$. A quasi-linear trend from heavier to lighter Mo isotopic composition can be identified within the first few metres in both basins. The slopes of the two regression lines through these data differ by a factor of seven. Assuming a common environmental process to be responsible for the decline observed in both basins, a sedimentation rate that is seven times higher in Oman than in South China would be the most straightforward explanation. If the complete sections are correspondingly scaled by this factor, a covariance of Mo isotopes is also found for the remaining stratigraphy (Fig. 1). This assumption is supported by the decrease in uranium and vanadium abundances stratigraphically upwards from the PC/C boundary, which indicates a sedimentation rate for Oman^{7,16} that is five to ten times higher than that for South China (see Supplementary Information for details). The scaled and combined Mo isotopic signal (Fig. 1) indicates a transient Mo signal immediately following the PC/C boundary, most likely resulting from a brief, global, non-steady state situation within the earliest Cambrian ocean.

The palaeoenvironmental implications of this Early Cambrian transient Mo isotope signal can be evaluated by modelling the Mo oceanic inventory in relation to the Mo fluxes. The Mo seawater composition can be adequately estimated by adjusting the Mo sedimentary fluxes in a first-order box model of the Mo oceanic cycle. We divided the Mo output into variable proportions of a strong euxinic output (reflecting the seawater Mo isotopic composition) and a light output (with a Mo signature that is $-2\delta^{98/95}\text{Mo}$ lighter than sea water). The latter model parameter represents the sum of oxic, suboxic

and even slightly euxinic Mo sedimentations, all of which are known to incorporate Mo isotopic compositions lower than that of coexisting sea water^{17,18}. Which of these light sinks is dominant is to be deduced from the geological context (see below). Under steady-state conditions the oceanic Mo input (oxic continental weathering) must equal its output. We have also assumed Mo input values and the Mo abundance in sea water to be the same as today's values. Changing these parameters would result in a change of absolute model timescales. However, relative timescales and processes would remain unaffected.

The necessary conditions to mimic the transient Mo signal are shown in two model runs in Fig. 2. In both scenarios, the Mo ocean inventory is depleted on a very short timescale owing to a euxinic Mo output increased by a factor of more than 150 relative to the previous steady state. This strong depletion of the Mo ocean inventory is necessary to make the Mo isotopic composition of the continental Mo influx ($\sim 0.2\delta^{98/95}\text{Mo}$) the dominant signature for a short time as observed in the large negative $\delta^{98/95}\text{Mo}$ peak shortly after the PC/C boundary. Another requirement is the short timescale of this euxinic output. Both model results show that the sudden increase in the euxinic output is followed by an exponential decline, which returns the Mo euxinic output to steady-state values within around 250,000 yr. A disruption of the Mo oceanic steady-state situation as a result of this short, but intense, Mo euxinic output accounts for the fluctuation of the Mo signal on such short timescales.

To reconcile the two positive Mo isotopic excursions seen in the Mo isotopic data set, an additional 30-times-increased light Mo output has to be implemented in the model (Fig. 2b). The combination of the increased Mo euxinic output together with the increased light/suboxic fractionation results in Mo depletion and a heavy isotopic composition of the ocean inventory shortly after the PC/C boundary. The probable cause for the second positive Mo excursion is a slower decline in the light/suboxic sedimentation in comparison with the euxinic sedimentation.

Our model results for the Mo isotopic transient signal have two main implications consistent with the metal enrichments found at the PC/C boundary. First, the strong increase in the euxinic output

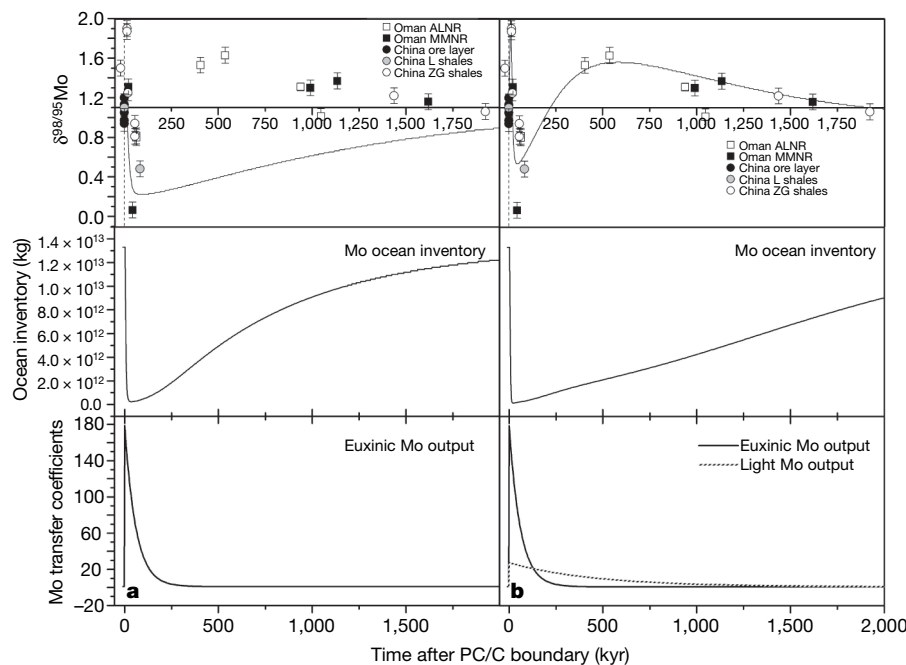


Figure 2 | The modelled Mo isotopic seawater signature in comparison with measured black shale isotope Mo data. Stratigraphic positions of the shale samples were recalculated into deposition time after the PC/C boundary, taking higher authigenic sedimentation rates shortly after the PC/C boundary into account. **a**, The modelled $\delta^{98/95}\text{Mo}$ curve taking only

increased euxinic Mo sedimentation into account. **b**, The modelled $\delta^{98/95}\text{Mo}$ curve with increased euxinic and light Mo output. A light Mo output of $-2\delta^{98/95}\text{Mo}$ was used (see Supplementary Information for details). Error bars show the external standard reproducibility of $0.1\delta^{98/95}\text{Mo}$ if measured uncertainties are lower.

together with its fast exponential decline are in accord with the notion of a short but intense upwelling of euxinic bottom-water masses that would have dramatically lowered the Mo ocean inventory. Variations in the carbon isotopic signal ($\delta^{13}\text{C}$) at the PC/C boundary indicate non-steady-state processes on short timescales ($<100,000\text{ yr}$)¹⁹, which is in good agreement with our modelled upwelling time range. A concurrent increase in weakly euxinic to suboxic sedimentary conditions, manifest in an isotopically light Mo output, can be expected in upwelling regions owing to the mixture of bottom-water H_2S and oxic near-surface waters and the oxidation of H_2S at the water–atmosphere interface.

This picture is consistent with other prominent geological and geochemical features at the PC/C boundary, such as the negative $\delta^{13}\text{C}$ excursion and the global accumulation of large phosphorite deposits²⁰. Organic matter sinking into the anoxic bottom-water zone resulted in the build-up of a dissolved phosphate and isotopically light organic carbon repository²¹. The destabilization of the oceanic chemocline²², possibly caused by a previous increase in oxygen levels²³ or by a change in ocean circulation patterns, could have brought these anoxic bottom-water masses to shelf regions containing free oxygen. Oxidation would have released phosphorus, which was then predominantly mineralized²⁴. Subsequently, the isotopically light carbon supply into shelf regions was probably responsible for the prominent negative $\delta^{13}\text{C}$ excursion.

The fact that most Ediacaran fossils have no post-Proterozoic record and that Early Cambrian trace and body fossils appear over only a protracted interval in the Cambrian suggests that the Cambrian fauna did not simply succeed the Ediacaran biota²⁵. This time gap lends substance to the hypothesis that the Ediacaran and Cambrian faunas are separated by an event of mass extinction. Several palaeoclimatic, palaeoenvironmental and palaeoecological reasons can be responsible for mass extinctions in general²⁶. These include catastrophic methane release²⁷, large-scale volcanism (both of which would lead to global warming and hypercapnia), and hydrogen sulphide poisoning due to upwelling euxinic bottom waters. Of these, hydrogen sulphide poisoning is the only process that can account for the observed Early Cambrian Mo isotope signal and provide a plausible explanation for the sudden extinction of the Ediacaran fauna. It is well established that hydrogen sulphide is almost universally toxic to eukaryotic cells in micromolar or higher concentrations^{22,28}. Increasing oxygenation of the upper ocean and atmosphere following the Marinoan glaciation is thought to have triggered the development of the Ediacaran fauna²³, and to have caused destabilization of the oceanic chemocline²³. As a consequence, upwelling euxinic bottom water is likely to have rapidly poisoned the Ediacaran fauna.

METHODS SUMMARY

Sample powders were oxidized at $800\text{ }^\circ\text{C}$ for $\sim 8\text{ h}$. The equivalent of $\geq 50\text{ ng Mo}$ was put in a Teflon beaker together with 6 M HCl and heated to $\sim 100\text{ }^\circ\text{C}$ for $\sim 24\text{ h}$. The supernatant was decanted into a second beaker containing the necessary amount of ^{97}Mo – ^{100}Mo double spike. The remaining sample material was dried and attacked with concentrated HF and HNO_3 (4:1) at $\sim 100\text{ }^\circ\text{C}$. After complete dissolution and evaporation, the residue was redissolved in 6 M HCl and added to the second beaker. After evaporation, the material was taken up in $4\text{ M HCl} + \text{H}_2\text{O}_2$ and loaded onto an anion exchange resin to wash out cations. The molybdate anion was finally eluted with 2 M HNO_3 . A subsequent cation exchange column separated Mo from residual Fe and Zr. Samples were measured as 0.5 M HNO_3 solution on a Nu Instruments MC-ICP-MS equipped with an ESI Apex nebulizer. The external standard reproducibility was $0.1\delta^{98/95}\text{Mo}$ (2 s.d.)⁴ (see Supplementary Information).

Received 18 July 2007; accepted 9 May 2008.

Published online 28 May 2008.

1. Brasier, M. Background to the Cambrian Explosion. *J. Geol. Soc. Lond.* **149**, 585–587 (1992).
2. Grotzinger, J., Bowring, S., Saylor, B. & Kaufman, A. Biostratigraphic and geochronologic constraints on early animal evolution. *Science* **270**, 598–604 (1995).

3. Amthor, J. *et al.* Extinction of Cloudina and Namacalathus at the Precambrian–Cambrian boundary in Oman. *Geology* **31**, 431–434 (2003).
4. Siebert, C., Nagler, T., von Blanckenburg, F. & Kramers, J. Molybdenum isotope records as a potential new proxy for paleoceanography. *Earth Planet. Sci. Lett.* **211**, 159–171 (2003).
5. Siebert, C., Kramers, J., Meisel, P. & Nagler, T. PGE, Re–Os and Mo isotope systematics in Archean and early Proterozoic sedimentary systems as proxies for redox conditions of the early Earth. *Geochim. Cosmochim. Acta* **69**, 1787–1801 (2005).
6. Arnold, G., Anbar, A., Barling, J. & Lyons, T. Molybdenum isotope evidence for widespread anoxia in mid-Proterozoic oceans. *Science* **304**, 87–90 (2004).
7. Schroder, S. & Grotzinger, J. Evidence for anoxia at the Ediacaran–Cambrian boundary: The record of redox sensitive trace elements and rare earth elements in Oman. *J. Geol. Soc. Lond.* **164**, 175–187 (2007).
8. Amthor, J., Ramseyer, K., Faulkner, T. & Lucas, P. Stratigraphy and sedimentology of a chert reservoir at the Precambrian–Cambrian Boundary: the Al Shomou silicilyte, South Oman Salt Basin. *GeoArabia* **10**, 89–122 (2005).
9. Lehmann, B. *et al.* Highly metalliferous carbonaceous shale and Early Cambrian seawater. *Geology* **35**, 403–406 (2007).
10. Mao, J. *et al.* Re–Os dating of polymetallic Ni–Mo–PGE–Au mineralization in Lower Cambrian black shales of South China and its geological significance. *Econ. Geol.* **97**, 1051–1061 (2002).
11. Cao, S., Ma, D. & Pan, J. Stable isotopic geochemistry of organic carbon and pyrite sulfur from the Early Cambrian black shales in Northwestern Hunan China. *Prog. Nat. Sci.* **14**, 181–187 (2004).
12. Steiner, M., Wallis, E., Erdtmann, B.-D., Zhao, Y. & Yang, R. Submarine-hydrothermal exhalative ore layer in black shales from South China and associated fossils – insights into Lower Cambrian facies and bio-evolution. *Palaeogeogr. Palaeoclimatol. Palaeoecol.* **169**, 165–191 (2001).
13. Algeo, J. & Lyons, T. Mo–total organic carbon covariation in modern anoxic marine environments: Implications for analysis of paleoredox and paleohydrographic conditions. *Paleoceanography* **21**, 1–23 (2006).
14. Erickson, B. & Helz, G. Molybdenum(VI) speciation in sulfidic waters: Stability and lability of thiomolybdates. *Geochim. Cosmochim. Acta* **64**, 1149–1158 (2000).
15. Banerjee, D., Schidlowski, M., Siebert, F. & Brasier, M. Geochemical changes across the Proterozoic–Cambrian transition in the Durmala phosphorite mine section, Mussoorie Hills, Garhwal Himalaya, India. *Palaeogeogr. Palaeoclimatol. Palaeoecol.* **132**, 183–194 (1997).
16. Pan, J., Ma, D. & Cao, S. Trace element geochemistry of the Lower Cambrian black rock series from northwestern Hunan, South China. *Prog. Nat. Sci.* **14**, 64–70 (2004).
17. Siebert, C., McManus, J., Bice, A., Poulson, R. & Berelson, W. Molybdenum isotope signatures in continental margin marine sediments. *Earth Planet. Sci. Lett.* **241**, 723–733 (2006).
18. Nagler, T., Siebert, C., Luschen, H. & Bottcher, M. Sedimentary Mo isotope record across the Holocene fresh-brackish water transition of the Black Sea. *Chem. Geol.* **219**, 283–295 (2005).
19. Maloof, A., Schrag, D., Crowley, J. & Bowring, S. An expanded record of Early Cambrian carbon cycling from the Anti-Atlas Margin, Morocco. *Can. J. Earth Sci.* **42**, 2195–2216 (2005).
20. Cowie, J. & Brasier, M. (eds) *The Precambrian–Cambrian Boundary* (Clarendon, Oxford, UK, 1989).
21. Shen, Y., Schidlowski, M. & Chu, X. Biogeochemical approach to understanding phosphogenic events of the terminal Proterozoic to Cambrian. *Palaeogeogr. Palaeoclimatol. Palaeoecol.* **158**, 99–108 (2000).
22. Kump, L., Pavlov, A. & Arthur, M. Massive release of hydrogen sulfide to the surface ocean and atmosphere during intervals of ocean anoxia. *Geology* **33**, 397–400 (2005).
23. Fike, D. A., Grotzinger, J. P., Pratt, L. M. & Summons, R. E. Oxidation of the Ediacaran Ocean. *Nature* **444**, 744–747 (2006).
24. Mort, H. *et al.* Phosphorus and the role of productivity and nutrient recycling during oceanic anoxic event 2. *Geology* **35**, 483–486 (2007).
25. Knoll, A. & Carroll, S. Early animal evolution: Emerging views from comparative biology and geology. *Science* **284**, 2129–2137 (1999).
26. Twitchett, R. The paleoclimatology, paleoecology and paleoenvironmental analysis of mass extinction events. *Palaeogeogr. Palaeoclimatol. Palaeoecol.* **131**, 190–213 (2006).
27. Kirschvink, J. & Raub, T. A methane fuse for the Cambrian explosion: carbon cycles and true polar wander. *C.R. Geosci.* **335**, 65–78 (2003).
28. Knoll, A., Bambach, R., Payne, J., Pruss, S. & Fischer, W. Paleophysiology and end-Permian mass extinction. *Earth Planet. Sci. Lett.* **256**, 295–313 (2007).

Supplementary Information is linked to the online version of the paper at www.nature.com/nature.

Acknowledgements This work was financed by grants from the Swiss National Foundation to J.D.K. and T.F.N., from Deutsche Forschungsgemeinschaft to B.L., and from the German Academic Exchange Service to S.S. Thanks to Petroleum Development Oman LLC for financial and logistical support, and to J. Grotzinger and NASA for initial analytical work.

Author Information Reprints and permissions information is available at www.nature.com/reprints. Correspondence and requests for materials should be addressed to M.W. (martin.wille@anu.edu.au).